Scientific Research and Essay Vol. 4 (4), pp. 328-345, April, 2009
Available online at http://www.academicjournals.org/SRE
ISSN 1992-2248 © 2009 Academic Journals

Full Length Research Paper

Non-planar coupled shear walls with stiffening beams

E. Emsen[1*], C. D. Turkozer[2], O. Aksogan[2], R. Resatoglu[3] and M. Bikçe[4]

[1]Department of Civil Engineering, Akdeniz University, 07058, Antalya, Turkey.
[2]Department of Civil Engineering, University of Cukurova, 01330, Adana, Turkey.
[3]Department of Civil Engineering, Near East University, Nicosia, North Cyprus, Turkey.
[4]Department of Civil Engineering, Mustafa Kemal University, 31024 Hatay, Turkey.

Accepted 17 February, 2009

This paper concerns itself with the static analysis of non-planar coupled shear walls with any number of stiffening beams. Furthermore, the change of the heights of the stories and connecting beams from region to region along the height are taken into consideration. The stiffening of coupled shear walls is realized by placing high connecting beams at the levels of whole or partial stories used as storage or service areas. The analysis is based on Vlasov's theory of thin-walled beams and Continuous Connection Method (CCM). In the analysis, the compatibility equation has been written at the midpoints of the connecting and stiffening beams. The method of analysis presented was compared with the SAP2000 structural analysis program. The results obtained showed good agreement, verifying the accuracy of the proposed method, which can efficiently be used for the pre-design computations of tall buildings.

Key words: Static analysis, continuous connection method, coupled shear wall, stiffening beam, non-planar, warping deformation.

INTRODUCTION

In multi-storey buildings made of reinforced concrete, lateral loads are often resisted by specially arranged shear walls. Shear wall components may be planar, are usually located at the sides of the building or in the form of a core which houses staircases or elevator shafts. Weakening of shear walls in tall buildings by doors, windows and corridor openings is one of the most frequently encountered problems of structural engineering. When the coupling action between the piers separated by openings becomes important, some of the external moment is resisted by the couple formed by the axial forces in the walls due to the increase in the stiffness of the coupled system by the connecting beams. Actually, the deformation of a coupled shear wall subjected to lateral loading is not confined to its plane. Studies considering in-plane, out-of-plane and torsional deformations in the investigation of coupled shear walls are called non-planar coupled shear wall analyses. In non-planar coupled shear walls, both the flexural and torsional behaviours under external loading have to be taken into account in the analysis. When thin-walled structures are twisted, there is a so-called warping of the cross-section and the Bernoulli-Navier hypothesis is violated. The warping of shear walls is greatly restrained by the floor slabs and the foundations. A classical analysis of warping torsion requires the prior evaluation of the shear centre location, the principal sectorial area diagram, the warping moment of inertia and the torsion constant (Zbirohowski, 1967).

When the height restrictions prevent connecting beams from fulfilling their tasks of reducing the maximum total shear wall bending moments at the bottom and the maximum lateral displacements at the top, beams with high moments of inertia, called "stiffening beams", are placed at certain heights to make up for this deficiency. Stiffening of coupled shear walls decreases the lateral displacements, thus, rendering an increase in the height of the building possible. Hence, assigning some stories of the building as storages, service areas and the like and placing high beams on those floors seems to be a logical solution. Such coupled shear walls are called "stiffened coupled shear walls". Such beams can be steel trusses or reinforced concrete beams of very high bending stiff-

*Corresponding author. E-mail: eemsen@akdeniz.edu.tr. Tel: +90-0242-3106385. Fax: +90-0242-3106306.

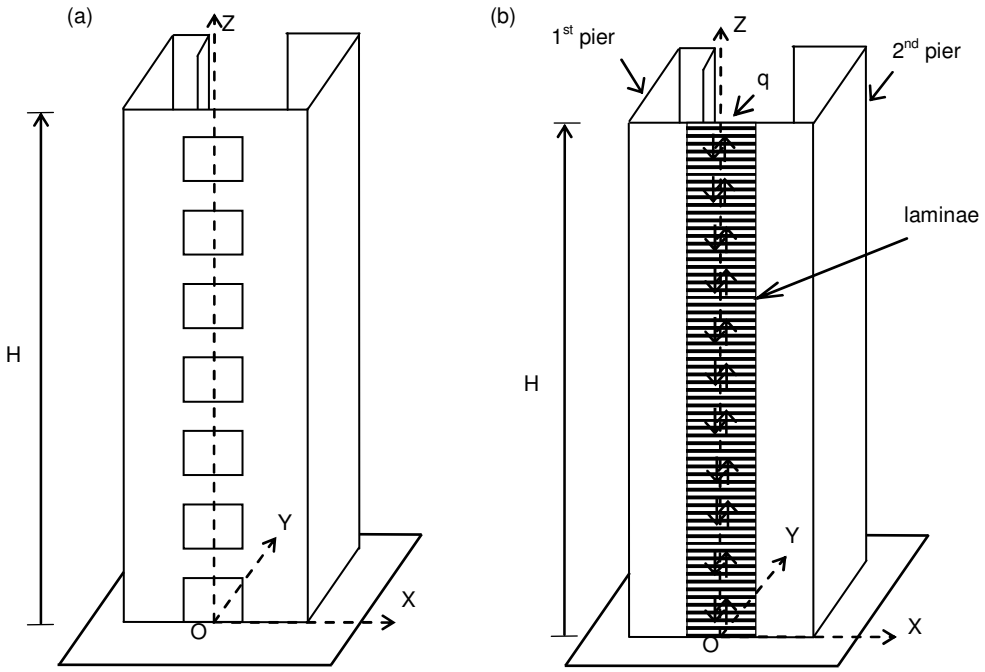

Figure 1. Non-planar coupled shear wall and equivalent structure.

ness.

All of the analyses in the literature on stiffened coupled shear walls concern themselves with planar coupled shear walls (Aksogan et al., 1993; Arslan et al., 2004; Aksogan et al., 2007). No study has been made, to the knowledge of the authors, concerning the static analysis of stiffened non-planar coupled shear walls, so far.

In the present work, the static analysis of non-planar coupled shear walls with any number of stiffening beams, is carried out which is applicable for asymmetric structural systems as well as symmetric ones on rigid foundation. The analysis is based on the Continuous Connection Method (CCM), in conjunction with Vlasov's theory (1961) of thin-walled beams, following an approach similar to the one used by Tso and Biswas (1973). In the CCM, the connecting beams are assumed to have the same properties and spacing along the entire height of the wall. The discrete system of connecting beams is replaced by continuous laminae of equivalent stiffness (Rosman, 1964). CCM has been employed in the analysis and the compatibility equation has been written at the mid-points of the connecting beams. For this purpose, the connecting beams have been replaced by an equivalent layered medium. The axial force in the piers is determined from the differential equation which is obtained by using the compatibility and equilibrium equations. Then, all relevant quantities of the problem are determined employing their expressions in terms of the axial force.

The present formulation is implemented with a Fortran Computer program. Using this computer program an asymmetrical example has been solved and compared with the solutions found by the SAP2000 (MacLeod et al., 1977; Wilson, 1997) structural analysis program and a perfect match has been observed.

ANALYSIS

In this study, based on Vlasov's theory of thin walled beams and the CCM, an approximate method is presented for the analysis of non-planar coupled shear wall structures. The deformation of a coupled shear wall subjected to a lateral loading is not always confined to its plane. For this reason, the present analysis is a three dimensional analysis of coupled shear walls (Figure 1a). The CCM was developed by assuming that the discrete system of connections, in the form of individual coupling beams or floor slabs, could be replaced by continuous laminae as shown in Figure 1b.

The basic assumptions of the CCM for non-planar coupled shear walls can be summarized as follows:

- The geometric and material properties are constant throughout each region i along the height.
- Vlasov's theory for thin-walled beams of open section is valid for each pier.
- The walls and beams are assumed to be linearly elastic.
- The outline of a transverse section of the coupled shear wall at a floor level remains unchanged in plan (due to the rigid diaphragm assumption for floors). Moreover, the parts of the shear wall between floor levels are also assumed to satisfy this condition. Depending on the foregoing assumption, the axis of each connecting beam re-

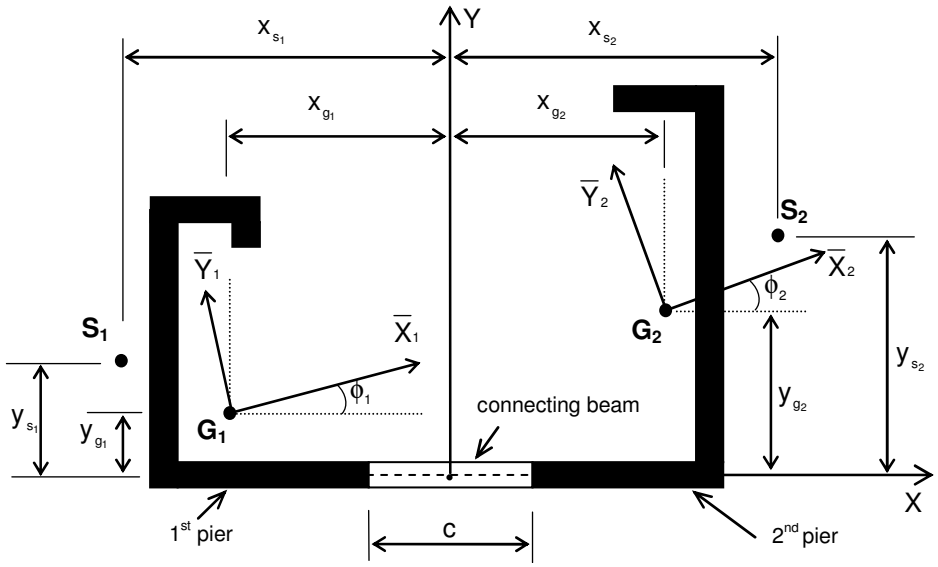

Figure 2. Plan of non-planar coupled shear wall in region i.

mains straight in plan and does not change its length. Furthermore, the slope and curvature at the ends of a connecting beam in the vertical plane are also assumed to be equal. Consequently, it can be proved in a straight forward manner that, depending on the fact that there are no vertical external forces on the connecting beams, their mid-points are points of contraflexure.

- The discrete set of connecting beams with bending stiffness EI_{ci} in region i are replaced by an equivalent continuous connecting medium of flexural rigidity EI_{ci}/h_i per unit length in the vertical direction.
- The discrete shear forces in the connecting beams in region i are replaced by an equivalent continuous shear flow function q_i, per unit length in the vertical direction along the mid-points of the connecting laminae.
- The torsional stiffness of the connecting beams is neglected.
- Bernoulli-Navier hypothesis is assumed to be valid for the connecting and stiffening beams.

A non-planar coupled shear wall and its plan for one region are given in Figures 2-3 with global axes OX, OY and OZ, the origin being at the mid-point of the clear span in the base plane. The X axis is parallel to the longitudinal direction of the connecting beams. The Z axis is the vertical axis and the Y axis is such that it completes an orthogonal right-handed system of axes. During the deformation, the outline of a transverse section of the shear wall remains unchanged (Figure 2).

Referring to the axes OX and OY, the coordinates of the centroids of the piers are taken to be (x_{g_1}, y_{g_1}) and (x_{g_2}, y_{g_2}), respectively. Throughout this study, the subscripts 1 and 2 express the left and the right piers, respectively. The subscript i $(i = 1,2,...,n)$, refers to the number of a region. Similarly, the shear centers of the piers are located at (x_{s_1}, y_{s_1}) and (x_{s_2}, y_{s_2}), respectively. The coordinates referred to the principal axes of pier j $(j = 1,2)$ which are represented by $(\overline{X}_j, \overline{Y}_j)$, making an angle ϕ_j with the respective global axes are shown in Figure 2. The $\overline{Z}_j$ axis is parallel to the global Z axis.

The axial force in each pier is found by writing down the vertical force equilibrium equation for the part of one pier above any horizontal cross-section as

$$T_i = \int_z^{z_i} q_i dz + \sum_{t=1}^{i-1} \left(\int_{z_{t+1}}^{z_t} q_t dz \right) + \sum_{t=1}^{i} V_t \qquad (i = 1,2,...,n) \qquad (1)$$

where V_i is the shear force in i^{th} stiffening beam. A cut through the points of contra-flexure of laminae exposes the shear flow q_i. The vertical force equilibrium of a dz element of one pier yields the relation

$$q_i = -T_i' \qquad (i = 1,2,...,n) \qquad (2)$$

Where a prime denotes differentiation with respect to z.

Compatibility equations

While obtaining the compatibility equations in a non-planar coupled shear wall analysis, it is assumed that all rows of connecting laminae will be cut through the mid-points, which are the points of zero moment.

The vertical displacement due to bending can be obtainedas the product of the slope at the section considered and the perpendicular distance of the point on Z axis from the respective neutral axis. In addition, vertical displacement arises, also, due to the twisting of the piers, and is

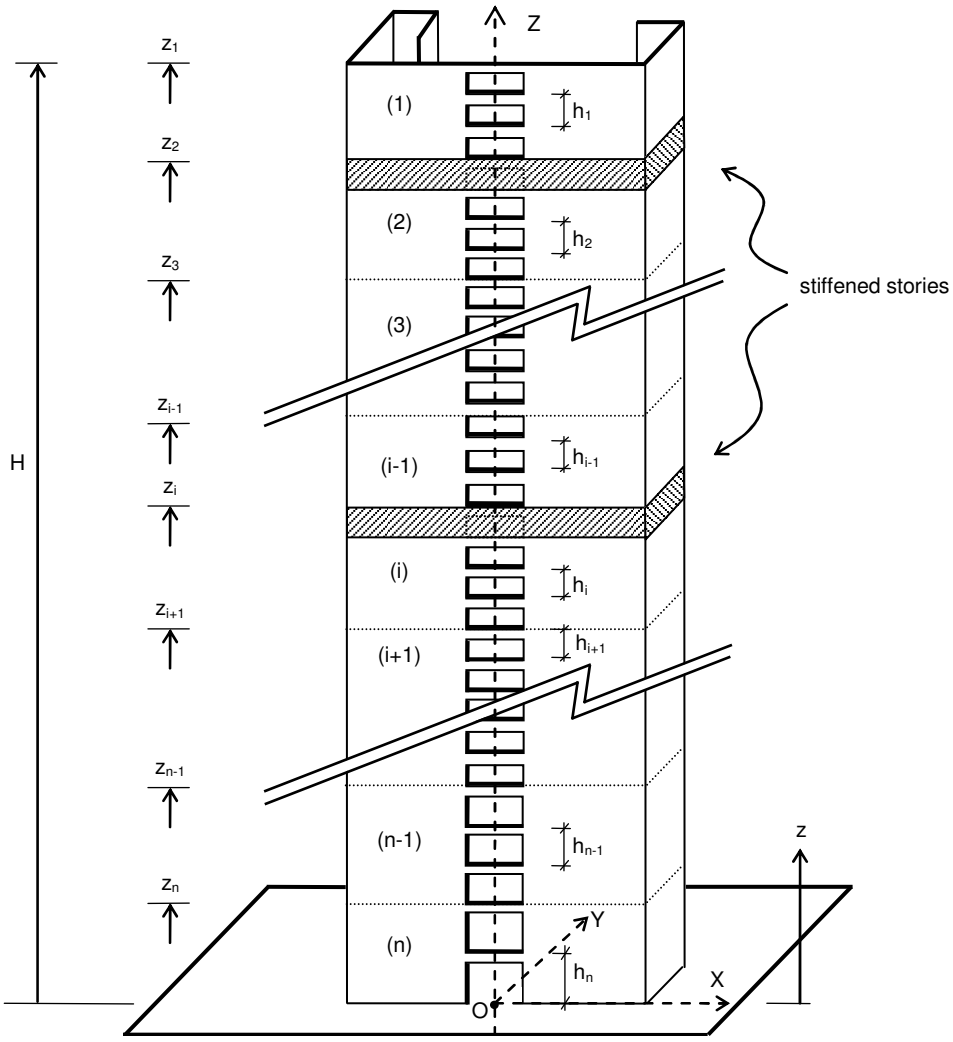

Figure 3. Non-planar stiffened coupled shear wall.

and is equal to the value of the twist at the section considered, times the sectorial area, ω, at the point on Z axis. Therefore, the total relative vertical displacement due to the deflections and rotations of the piers, can be written as

$$\delta_{1i} = \left(u'_{2i}\bar{x}_{g_2} - u'_{1i}\bar{x}_{g_1}\right) + \left(v'_{2i}\bar{y}_{g_2} - v'_{1i}\bar{y}_{g_1}\right) - \left(\theta'_{2i}\omega_2 - \theta'_{1i}\omega_1\right) \qquad (3)$$

The first two terms in equation (3) represent the contributions of the bending of the piers about the principal axes and the last represents the contribution of the twisting of the piers. ω_1 and ω_2 are the sectorial areas at points just to the left and the right of the cut for piers 1 and 2, respectively.

The local displacements u_{ji}, v_{ji} and θ_{ji} ($j = 1,2$, $i = 1,2,...,n$) and 2 may be expressed in terms of the global displacements u_i, v_i and θ_i by substituting expressions (4) into (3) and rearranging, yields

$$\delta_{1i} = u'_i a + v'_i b + \theta'_i(\omega + d) \qquad (5)$$

in which

$$\omega = \omega_1 - \omega_2 \qquad (6)$$

$$a = x_{g_2} - x_{g_1} \qquad b = y_{g_2} - y_{g_1}$$

$$d = x_{s_2}y_{g_2} - y_{s_2}x_{g_2} + y_{s_1}x_{g_1} - x_{s_1}y_{g_1} \qquad (7)$$

(7)For the compatibility of displacements, the relative vertical displacements of the cut ends must be equal to zero. Hence,

$$u'_i a + v'_i b + \theta'_i(\omega + d) - \frac{1}{E}\sum_{j=i+1}^{n}\left[\left(\frac{1}{A_1} + \frac{1}{A_2}\right)\int_{z_{j+1}}^{z_j} T_j\, dz\right]$$

$$- \frac{1}{E}\left(\frac{1}{A_1} + \frac{1}{A_2}\right)\int_{z_{i+1}}^{z} T_i\, dz + \frac{T'_i}{E}\left[\frac{h_i c^3}{12\, EI_{c_i}} + \frac{1.2\, h_i c}{GA_{c_i}}\right] = 0 \qquad (8)$$

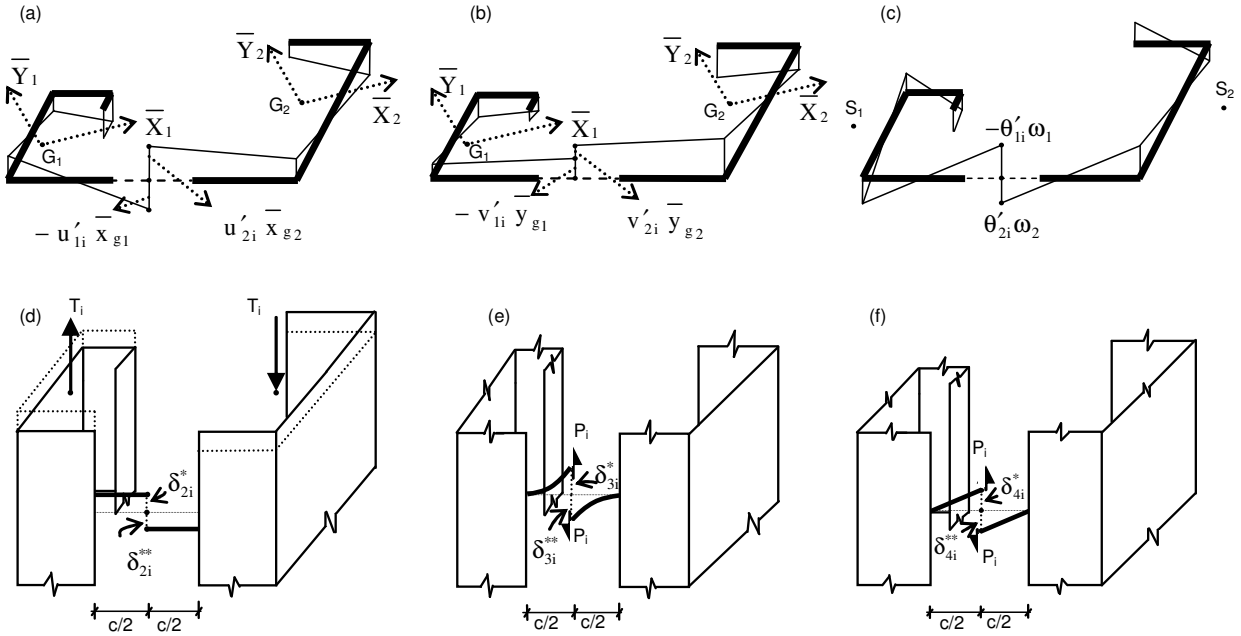

Figure 4. Relative vertical displacements at the mid-point of a lamina.

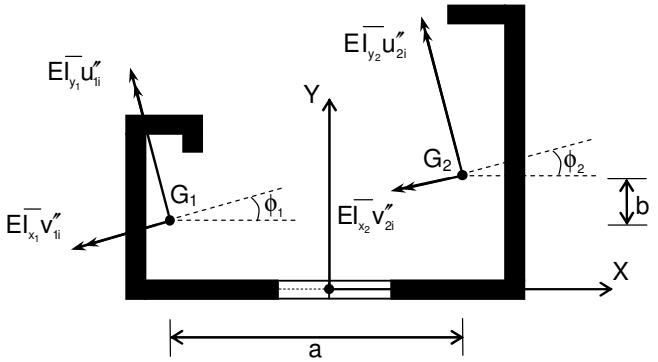

Figure 5. Internal bending moments.

Differentiating this equation with respect to z and letting

$$\theta_{ji} = \theta_i \qquad u_{ji} = u_i - y_{s_j}\theta_i \qquad v_{ji} = v_i + x_{s_j}\theta_i \tag{4}$$

$$\gamma_i = \frac{h_i c^3}{12 EI_{c_i}} + \frac{1.2 h_i c}{GA_{c_i}} \tag{9}$$

the following equation is obtained:

$$u_i'' a + v_i'' b + \theta_i''(\omega + d) - \frac{1}{E}\left(\frac{1}{A_1} + \frac{1}{A_2}\right) T_i + \frac{T_i''}{E}\gamma_i = 0 \qquad (i = 1,2,...,n) \tag{10}$$

The successive terms in (8) represent the relative vertical displacements due to: (a) the bending about $\overline{X_1}$ and $\overline{X_2}$ axes, (b) the bending about $\overline{Y_1}$ and $\overline{Y_2}$ axes, (c) the rotations of the piers, (d) the axial deformation of the piers, (e) the bending deformation in the laminae, and (f) the shearing deformation in the piers, respectively, as seen in Figure 4.

In Figure 4, δ expresses the displacements pertaining to the left side with superscript (*) and to the right side with superscript (**) and the relative vertical displacement is found by adding the contributions from both sides.

Equilibrium equations

The coordinate system and positive directions of internal bending moments acting on the different components of the coupled shear wall are adapted as shown vectorially in Figure 5.

These internal moments, along with the couple produced by the axial force, T_i, balance the external bending moments M_{EX_i} and M_{EY_i}. For the equilibrium of the moments about X and Y axes, the following relationships can be derived using Vlasov's theory of thin walled beams:

$$E\left(\overline{I}_{y_1} u_{1i}'' \sin\phi_1 + \overline{I}_{x_1} v_{1i}'' \cos\phi_1 + \overline{I}_{y_2} u_{2i}'' \sin\phi_2 + \overline{I}_{x_2} v_{2i}'' \cos\phi_2\right) + T_i b - M_{EX_i} = 0 \tag{11}$$

$$E\left(\overline{I}_{y_1} u_{1i}'' \cos\phi_1 - \overline{I}_{x_1} v_{1i}'' \sin\phi_1 + \overline{I}_{y_2} u_{2i}'' \cos\phi_2 - \overline{I}_{x_2} v_{2i}'' \sin\phi_2\right) + T_i a - M_{EY_i} = 0 \tag{12}$$

In these equations, I_{x_j} and I_{y_j} are the second moments of area of the cross-sections, and I_{xy_j} is the product of inertia transformation equations for moments of inertia,

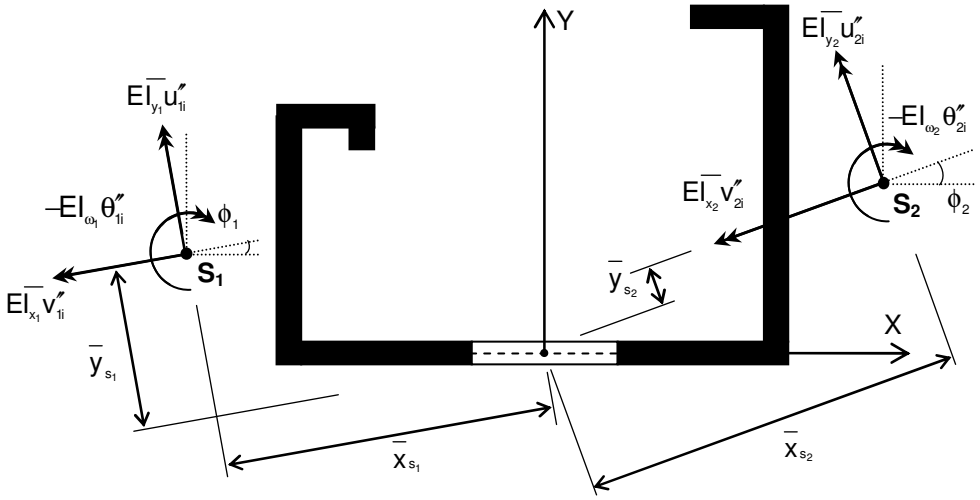

Figure 6. Internal bimoments and bending moments.

the moment components are found, in terms of the global of pier j (j=1, 2) about axes parallel to the global axes and passing through the centroids. $\bar{I}_{x_j}$ and $\bar{I}_{y_j}$ are the second moments of area of pier j ($j=1,2$) about its respective principal axes. On substituting the local displacement expressions given before in (4) into expressions (11-12) and applying the well-known displacements at the point on Z axis, as

$$M_{EX_i} = EI_{XY}u_i'' + EI_X v_i'' + EI_{\theta X}\theta_i'' + T_i b \qquad (i=1,2,...,n) \quad (13)$$

$$M_{EY_i} = EI_Y u_i'' + EI_{XY} v_i'' - EI_{\theta Y}\theta_i'' + T_i a \qquad (i=1,2,...,n) \quad (14)$$

where

$$I_X = I_{x_1} + I_{x_2} \quad I_Y = I_{y_1} + I_{y_2} \quad I_{XY} = I_{xy_1} + I_{xy_2} \quad (15)$$

$$I_{\theta X} = x_{s_1} I_{x_1} + x_{s_2} I_{x_2} - y_{s_1} I_{xy_1} - y_{s_2} I_{xy_2} \quad (16)$$

$$I_{\theta Y} = y_{s_1} I_{y_1} + y_{s_2} I_{y_2} - x_{s_1} I_{xy_1} - x_{s_2} I_{xy_2} \quad (17)$$

When non-planar coupled shear walls are rigidly constrained at the base, the cross-sections of the piers do not warp uniformly along the height and internal stresses evoke in the wall due to the bimoments. The internal force resultants shown in Figure 6 are caused by biaxial bending. These bending moments form bimoments with the resisting moments at the bottom of the wall and show up in the bimoment equilibrium equation.

In order to obtain the bimoment equilibrium equation, the coupled shear wall will be cut through by a horizontal plane such that an upper part is isolated from the lower part of the structure. The internal bimoments in the structure consist of two parts; one contributed by the individual piers (Figure 6) and the other due to the resistance of the connecting laminae and stiffening baems (Figure 7).

In Figure 6, the internal bimoment expressions $-EI_{\omega_{ji}}\theta''_{ji}$ (j=1,2, i=1,2,…,n), are caused by the non-uniform warping of the cross-sections of the piers. It must be mentioned that the computation of the internal bimoments created at the point on Z axis by the bending moments of the wall, are carried out after transferring the bending moments to the shear centers of the piers.

Let $\bar{B}_i$ be the resultant bimoment about Z axis, which is due to the resistance offered by the piers. It can be written as (Figure 6):

$$\bar{B}_i = -EI_{\omega_1}\theta''_{1i} - EI_{\omega_2}\theta''_{2i} + E\bar{I}_{y_1}u''_{1i}\left(\bar{y}_{s_1}\right) + E\bar{I}_{y_2}u''_{2i}\left(\bar{y}_{s_2}\right) + E\bar{I}_{x_1}v''_{1i}\left(-\bar{x}_{s_1}\right) - E\bar{I}_{x_2}v''_{2i}\left(\bar{x}_{s_2}\right) \quad (18)$$

Using the geometric relationship, the resultant resisting bimoment of the piers for all regions in the structure are found as:

$$\bar{B}_i = EI_{\theta Y}u_i'' - EI_{\theta X}v_i'' - EI_\omega\theta_i'' \qquad (i=1,2,...,n) \quad (19)$$

in which

$$I_\omega = I_{\omega_1} + I_{\omega_2} + x_{s_1}^2 I_{x_1} + x_{s_2}^2 I_{x_2} + y_{s_1}^2 I_{y_1} + y_{s_2}^2 I_{y_2} - 2x_{s_1}y_{s_1}I_{xy_1} - 2x_{s_2}y_{s_2}I_{xy_2} \quad (20)$$

In addition, there are bending moments $M_{xq_{1i}}$, $M_{yq_{1i}}$, $M_{xq_{2i}}$, and $M_{yq_{2i}}$ and bimoments $B_{q_{1i}}$ and $B_{q_{2i}}$, due to the summation of the shear forces in the laminae, as shown in Figures 7-8. All quantities are related to the shear centers of the piers, S_1 and S_2. In order to determine the bimoment due to the shear forces in the laminae, the relationship between the force components in the piers, may be determined from the free body diagram in Figure 7.

Let $\bar{\bar{B}}_i$ be the resultant bimoment due to the additional

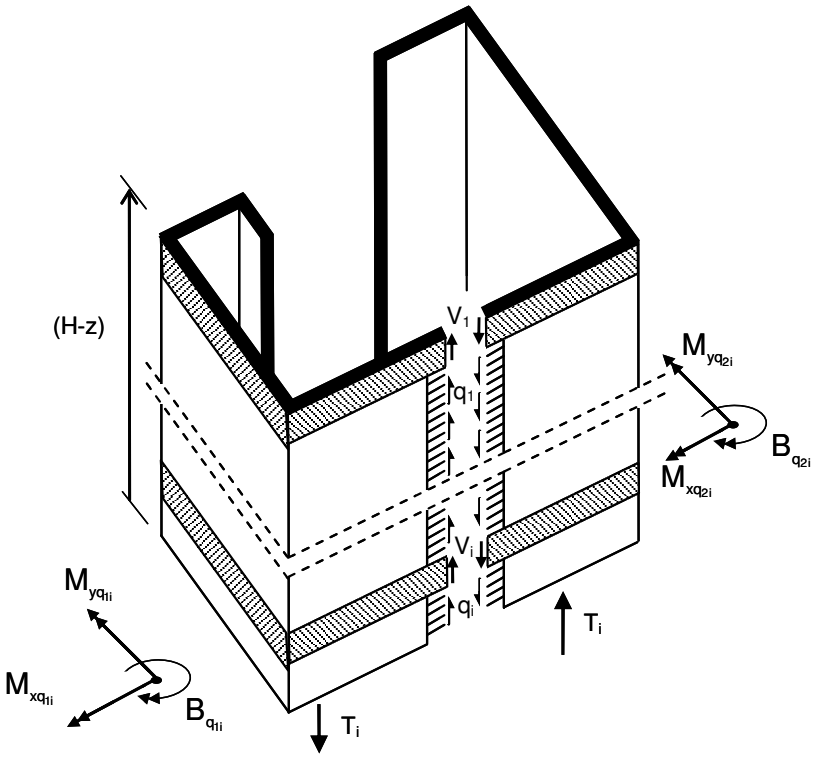

Figure 7. 3-D view of the additional internal bending moments and bimoments due to the shear forces in the connecting medium.

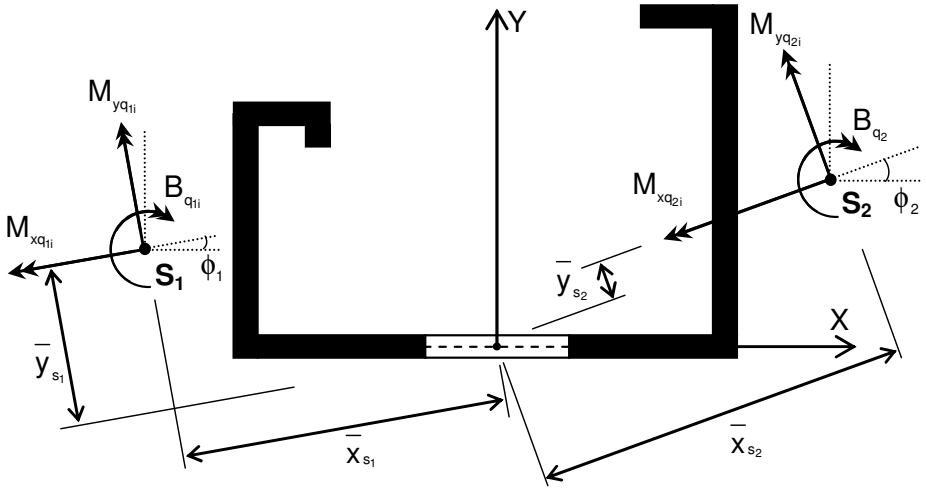

Figure 8. Cross-sectional view of the additional internal bending moments and bimoments due to the shear flow in the connecting medium.

bending moments and bimoments about Z axis, as shown in Figure 8.

The shear forces in the laminae produce bimoments on the piers. For each pier, the bimoment $B_{q_{ji}}$ is caused by T_i (instead of the summation of the shear flow in the connecting medium, see equation (1)), and is equal to the product of this force and the principal sectorial area ω_j of the point of its application. Therefore, for the two piers,

$$B_{q_{1i}} = -T_i\ \omega_1 \qquad B_{q_{2i}} = T_i\ \omega_2 \tag{21}$$

The resultant bimoment, $\overline{\overline{B}}_i$, due to these additional

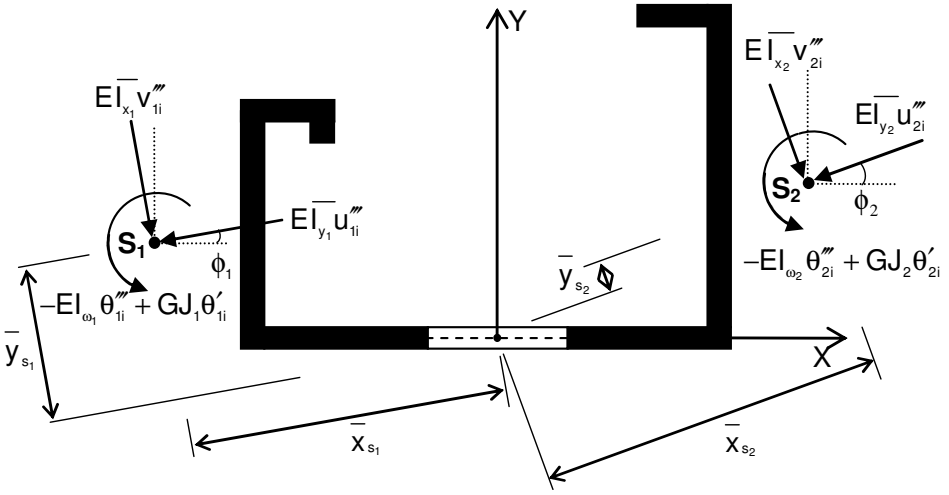

Figure 9. Internal twisting moments and shear forces.

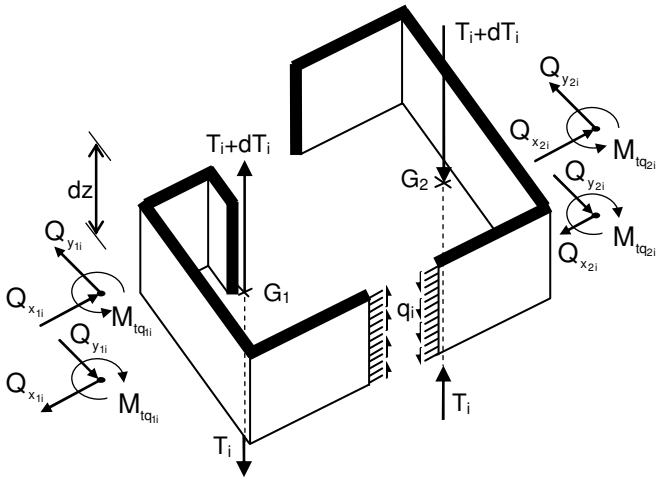

Figure 10. 3-D view of the additional internal shear forces and twisting moments due to the shear flow in the connecting medium.

bending moments and bimoments about Z axis, then, found as:

$$\overline{\overline{B}}_i = B_{q_{1i}} + B_{q_{2i}} + M_{xq_{1i}}\left(-\bar{x}_{s_1}\right) + M_{yq_{1i}}\left(\bar{y}_{s_1}\right) - M_{xq_{2i}}\left(\bar{x}_{s_2}\right) + M_{yq_{2i}}\left(\bar{y}_{s_2}\right) \qquad (22)$$

These additional bending moments and bimoments acting on an element are shown in Figure 8. From the consideration of equilibrium of the moments about $\overline{X}_1$ and $\overline{Y}_1$ axes for pier 1, the following relations can be obtained, respectively:

$$M_{xq_{1i}} + T_i\left(\bar{y}_{g_1}\right) = 0 \quad M_{yq_{1i}} - T_i\left(-\bar{x}_{g_1}\right) = 0 \qquad (23)$$

$$M_{xq_{1i}} = -T_i\,\bar{y}_{g_1} \qquad M_{yq_{1i}} = -T_i\,\bar{x}_{g_1} \qquad (24)$$

Similar consideration for the other pier gives

$$M_{xq_{2i}} = T_i\,\bar{y}_{g_2} \qquad M_{yq_{2i}} = T_i\,\bar{x}_{g_2} \qquad (25)$$

Substituting (21,24-25) in (22), using (7) and simplifying, the resultant bimoment, about the vertical axis through point O, due to the component bending moments and bimoments is found as:

$$\overline{\overline{B}}_i = -(\omega + d)T_i \qquad (i = 1,2,...,n) \qquad (26)$$

Equating the external bimoment, B_{E_i}, to the internal resisting bimoments, the bimoment equilibrium equation of the isolated part of the coupled shear wall above an arbitrary horizontal plane is established. Finally, the foregoing equilibrium equations for all regions of the structure can be written as follows:

$$B_{E_i} = \overline{B}_i + \overline{\overline{B}}_i \qquad (27)$$

$$B_{E_i} = EI_{\theta Y}u''_i - EI_{\theta X}v''_i - EI_\omega\theta''_i - (\omega + d)T_i \qquad (i = 1,2,...,n) \qquad (28)$$

In order to obtain the twisting moment equilibrium equation, the coupled shear wall will be cut through by a horizontal plane such that an upper free body diagram is isolated from the rest of the structure.

The internal twisting moments (torque) in the structure consist of two parts; one contributed by the individual piers as shown in Figure 9 and the other due to the resistance of the connecting laminae, in other words, the differential effect of the shear flow q_i in the connecting medium as shown in Figure 10.

In Figure 9, expressions $GJ_j\theta'_{ji}$ (j=1,2, i=1,2,…,n) are the St. Venant twisting moments. Expressions $-EI_{\omega_j}\theta'''_{ji}$ (j=1,2, i=1,2,…,n) are additional twisting moments due to the non-uniform warping (Zbirohowski, 1967) of the piers along the height. Furthermore, the total twisting moment

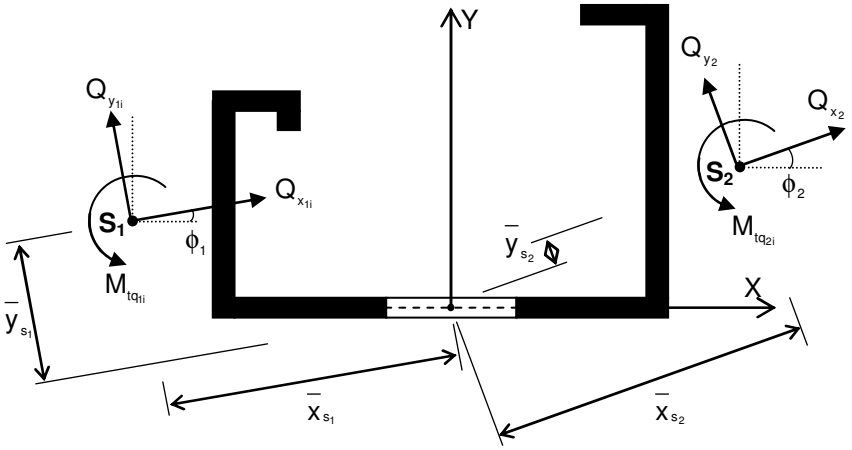

Figure 11. Cross-sectional view with the additional internal twisting moments and shear forces due to the shear flow q_i .

due to the shear forces in the cross-sections of the piers about Z axis must also be considered.

Let $\overline{M_{t_i}}$ be the resultant torque about Z axis, which is due to the resistance offered by the piers. It can be written as (Figure 9):

$$\overline{M_{t_i}} = GJ_1\theta'_{1i} + GJ_2\theta'_{2i} - EI_{\omega_1}\theta'''_{1i} - EI_{\omega_2}\theta'''_{2i} + E\overline{I_{y_1}}u'''_{1i}\left(\bar{y}_{s_1}\right) + E\overline{I_{y_2}}u'''_{2i}\left(\bar{y}_{s_2}\right) + E\overline{I_{x_1}}v'''_{1i}\left(-\bar{x}_{s_1}\right) - E\overline{I_{x_2}}v'''_{2i}\left(\bar{x}_{s_2}\right) \quad (29)$$

structure are found as:

$$\overline{M_{t_i}} = EI_{\theta Y}u'''_i - EI_{\theta X}v'''_i + GJ\theta'_i - EI_{\omega}\theta'''_i \qquad (i = 1,2,...,n) \quad (30)$$

in which

$$J = J_1 + J_2 \quad (31)$$

In addition, there are shear forces $Q_{x_{1i}}$, $Q_{y_{1i}}$, $Q_{x_{2i}}$, and $Q_{y_{2i}}$, and twisting moments $M_{tq_{1i}}$ and $M_{tq_{2i}}$, developed in the section due to the shear flow, q_i, in the laminae, as shown in Figures 10-11.

The bimoments, due to q_i in the two piers, are:

$$dB_{z_{1i}} = q_i\,dz\,\omega_1 \qquad dB_{z_{2i}} = -q_i\,dz\,\omega_2 \quad (32)$$

These bimoments produce the flexural twisting moments $M_{tq_{1i}}$ and $M_{tq_{2i}}$, related to the shear centers S_1 and S_2, respectively. Based on Vlasov's theory of thin-walled beams:

$$M_{tq_{1i}} = \frac{dB_{z_{1i}}}{dz} = q_i\,\omega_1 \qquad M_{tq_{2i}} = \frac{dB_{z_{2i}}}{dz} = -q_i\,\omega_2 \quad (33)$$

The resultant twisting moment, $\overline{\overline{M_{t_i}}}$, due to these additional torques and shear forces about Z axis is, then, found as:

$$\overline{\overline{M_{t_i}}} = M_{tq_{1i}} + M_{tq_{2i}} - Q_{x_{1i}}\left(\bar{y}_{s_1}\right) - Q_{y_{1i}}\left(-\bar{x}_{s_1}\right) - Q_{x_{2i}}\left(\bar{y}_{s_2}\right) + Q_{y_{2i}}\left(\bar{x}_{s_2}\right) \quad (34)$$

From the consideration of equilibrium of the moments about $\overline{X_1}$ and $\overline{Y_1}$ axes for pier 1, the following relations can be obtained, respectively:

$$Q_{x_{1i}}\,dz + q_i\,dz\,\bar{x}_{g_1} = 0 \qquad Q_{y_{1i}}\,dz + q_i\,dz\,\bar{y}_{g_1} = 0 \quad (35)$$

$$Q_{x_{1i}} = -q_i\,\bar{x}_{g_1} \qquad Q_{y_{1i}} = -q_i\,\bar{y}_{g_1} \quad (36)$$

Similar consideration for the other pier gives

$$Q_{x_{2i}} = q_i\,\bar{x}_{g_2} \qquad Q_{y_{2i}} = q_i\,\bar{y}_{g_2} \quad (37)$$

Substituting (33,36-37) in (34), using (7) and simplifying, the resultant twisting moment, about the vertical axis through point O, due to the component shears and torques, yield

$$\overline{\overline{M_{t_i}}} = (\omega + d)q_i \qquad (i = 1,2,...,n) \quad (38)$$

Equating the external twisting moment, M_{Et_i}, to the internal resisting moments, with opposite sense, the equilibrium equation of the isolated part of the coupled shear wall above an arbitrary horizontal plane is established. Finally, the foregoing equilibrium equation for all regions of the structure can be written as follows:

$$M_{Et_i} = \overline{M_{t_i}} + \overline{\overline{M_{t_i}}} \quad (39)$$

$$M_{Et_i} = EI_{\theta Y}u'''_i - EI_{\theta X}v'''_i + GJ_i\theta'_i - EI_{\omega}\theta'''_i - (\omega + d)T'_i \qquad (i = 1,2,...,n) \quad (40)$$

General solution for axial force

Using the compatibility equation (8) and the four equilibrium equations (13), (14), (28), and (40), the 4n unknowns of the problem, namely u_i, v_i, θ_i, and T_i, can be found under the applied loadings M_{EX_i}, M_{EY_i}, B_{E_i}, and M_{Et_i}. The elimination of u_i, v_i, and θ_i from equations (10,13-14,28,40) yields the following differential equation for T_i:

$$(\beta_{1i})T_i''' - (\beta_{2i})T_i'' + (\beta_{3i})T_i = -M_{EY_i}''\left(\bar{I}_\omega K_3 + K_1 r\right) - M_{EX_i}''\left(\bar{I}_\omega K_4 - K_2 r\right) + \frac{GJ}{E}\left(M_{EY_i}K_3 + M_{EX_i}K_4\right) + M_{Et_i}' r \qquad (41)$$

where

$$\beta_{1i} = \gamma_i \bar{I}_\omega \qquad \beta_{2i} = \frac{\bar{I}_\omega}{A} + \frac{GJ\gamma_i}{E} + r^2 \qquad \beta_{3i} = \frac{GJ}{EA} \qquad (42)$$

The geometrical quantities used in equation (41) are defined as follows:

$$K_1 = \frac{\left(I_X I_{\theta Y} + I_{XY} I_{\theta X}\right)}{\Delta} \qquad K_2 = \frac{\left(I_{XY} I_{\theta Y} + I_Y I_{\theta X}\right)}{\Delta}$$
$$K_3 = \frac{\left(aI_X - bI_{XY}\right)}{\Delta} \qquad K_4 = -\frac{\left(aI_{XY} - bI_Y\right)}{\Delta} \qquad (43)$$
$$r = \omega + d + aK_1 - bK_2 \qquad \bar{I}_\omega = I_\omega - I_{\theta X}K_2 - I_{\theta Y}K_1$$
$$\frac{1}{A} = \left[\frac{1}{A_1} + \frac{1}{A_2}\right] + aK_3 + bK_4 \qquad \Delta = \left(I_X I_Y - I_{XY}^2\right)$$

In equation (41), M_{EX_i} and M_{EY_i} are the external bending moments and M_{Et_i} is the external twisting moment about the respective global axes and can be written as:

$$M_{EX_i} = P_Y(H-z) + \frac{W_Y(H-z)}{2} \qquad M_{EY_i} = P_X(H-z) + \frac{W_X(H-z)}{2} \qquad (44)$$

$$M_{Et_i} = P_X(-d_{PY}) + P_Y(d_{PX}) + W_X(H-z)(-d_{WY}) + W_Y(H-z)(d_{WX})$$

where, P_X and P_Y are the concentrated forces, W_X and W_Y are the uniform loads in X and Y directions, d_{PX} and d_{PY} are the moment arms of the components of the concentrated force, d_{WX} and d_{WY} are the moment arms of the distributed force components from the point on Z axis, respectively. Substituting expressions (44) in (41) and solving the resulting differential equation, T_i is found as follows:

$$T_i = D_{1i}\,\mathrm{Sinh}[\alpha_{1i} z] + D_{2i}\,\mathrm{Cosh}[\alpha_{1i} z] + D_{3i}\,\mathrm{Sinh}[\alpha_{2i} z] + D_{4i}\,\mathrm{Cosh}[\alpha_{2i} z]$$
$$+ \frac{1}{2\beta_{3i}^2 E}\Big\{ 2\beta_{2i}GJ(K_3 W_X + K_4 W_Y)$$
$$+ \beta_{3i}\,\big[GJ(H-z)(2K_3P_X + 2K_4P_Y + HK_3W_X$$
$$+ HK_4W_Y - (K_3W_X + K_4W_Y)z)$$
$$- 2E\big(\bar{I}_\omega K_3 W_X - d_{WY} r W_X + K_1 r W_X$$
$$+ \bar{I}_\omega K_4 W_Y + d_{WX} r W_Y - K_2 r W_Y\big)\big]\Big\} \quad (i = 1,2,...,n) \qquad (45)$$

in which

$$\alpha_{1i} = \sqrt{\left(\frac{\beta_{2i} - \sqrt{\beta_{2i}^2 - 4\beta_{1i}\beta_{3i}}}{2\beta_{1i}}\right)} \qquad \alpha_{2i} = \sqrt{\left(\frac{\beta_{2i} + \sqrt{\beta_{2i}^2 - 4\beta_{1i}\beta_{3i}}}{2\beta_{1i}}\right)} \qquad (46)$$

Employing the boundary conditions to determine the integration constants, T_i can be obtained in a straightforward manner.

Determination of the Shear Forces in the Stiffening Beams

Before writing down the boundary conditions, the shear forces in the stiffening beams must be determined. For this purpose, compatibility equation (8) must be written both for section i at level z_i and the stiffening beam i and solved simultaneously. Thus, employing the definition

$$S_i = \frac{\left[\frac{1.2h_i c}{GA_{c_i}} + \frac{h_i c^3}{12EI_{c_i}}\right]}{\left[\frac{1.2c}{GA_{s_i}} + \frac{c^3}{12EI_{s_i}}\right]} \qquad (47)$$

the shear force in the i^{th} stiffening beam is found as follows:

$$V_i = -S_i T_i'\big|_{z=z_i} \qquad (i = 1,2,...,n) \qquad (48)$$

Boundary Conditions

To determine the integration constants in the single fourth order differential equation (41) the following 4n boundary conditions are employed:

1- The structure being rigidly fixed at the base ($z = 0$)

$$u_n\big|_{z=0} = v_n\big|_{z=0} = \theta_n\big|_{z=0} = 0 \qquad u_n'\big|_{z=0} = v_n'\big|_{z=0} = \theta_n'\big|_{z=0} = 0 \qquad (49)$$

Applying equation (8) at ($z = 0$) and using (49), the first boundary condition is:

$$T'_n\big|_{z=0} = 0 \tag{50}$$

2-From equation (40), substituting θ''_n , θ'''_n , u'''_n and v'''_n in terms of T_n and putting $\theta'_n\big|_{z=0} = 0$, the second boundary condition at the bottom ($z = 0$) is found as:

$$M_{Et_n} - I_{\theta Y}\left[\frac{\left(M'_{EY_n}I_X - M'_{EX_n}I_{XY}\right)}{\Delta} + \frac{K_1}{r}\left(-M'_{EY_n}K_3 - M'_{EX_n}K_4 + \frac{T'_n}{A} - \gamma_n T'''_n\right) - T'_n K_3\right]$$

$$+ I_{\theta X}\left[\frac{\left(M'_{EX_n}I_Y - M'_{EY_n}I_{XY}\right)}{\Delta} - \frac{K_2}{r}\left(-M'_{EY_n}K_3 - M'_{EX_n}K_4 + \frac{T'_n}{A} - \gamma_n T'''_n\right) - T'_n K_4\right]$$

$$+ \frac{I_\omega}{r}\left[-M'_{EY_n}K_3 - M'_{EX_n}K_4 + \frac{T'_n}{A} - \gamma_n T'''_n\right] + (\omega + d)T'_n = 0 \tag{51}$$

3-From the equilibrium of the vertical forces in each pier in the uppermost region of the shear wall

$$T_1 = \int_z^H q_1 dz + V_1 \tag{52}$$

Applying this equation for the uppermost position ($z = H$), the first term on the right dropping out, considering expression (48), the third boundary condition is found as follows:

$$T_1\big|_{z=H} = -S_1 T'_1\big|_{z=H} \tag{53}$$

4-Substituting u''_1 , v''_1 and θ''_1 in the bimoment expression (28) and applying it at the top ($z = H$) the fourth boundary condition is obtained as:

$$B_{E_1} - I_{\theta Y}\left[\frac{\left(M_{EY_1}I_X - M_{EX_1}I_{XY}\right)}{\Delta} + \frac{K_1}{r}\left(-M_{EY_1}K_3 - M_{EX_1}K_4 + \frac{T_1}{A} - \gamma_1 T''_1\right)\right.$$

$$\left. - T_1 K_3\right] + I_{\theta X}\left[\frac{\left(M_{EX_1}I_Y - M_{EY_1}I_{XY}\right)}{\Delta} - \frac{K_2}{r}\left(-M_{EY_1}K_3 - M_{EX_1}K_4 + \frac{T_1}{A}\right.\right.$$

$$\left.\left. - \gamma_1 T''_1\right) - T_1 K_4\right] + \frac{I_\omega}{r}\left[-M_{EY_1}K_3 - M_{EX_1}K_4 + \frac{T_1}{A} - \gamma_1 T''_1\right]$$

$$+ (\omega + d)T_1 = 0 \tag{54}$$

5- From the vertical force equilibrium of one piece of the stiffening beam in either of the piers at height $z = z_i$

$$T_{(i-1)}\big|_{z=z_i} + V_i = T_i\big|_{z=z_i} \tag{55}$$

Substituting (48) in (55), the fifth type boundary condition is obtained as follows:

$$T_{(i-1)}\big|_{z=z_i} - S_i T'_i\big|_{z=z_i} = T_i\big|_{z=z_i} \qquad (i = 1,2,...,n) \tag{56}$$

6-Applying the compatibility equation (8) for two neighbouring regions (i) and (i–1) at height $z = z_i$, the following equation is obtained as the sixth type boundary condition:

$$T'_{(i-1)}\big|_{z=z_i}\left(\frac{1.2h_{(i-1)}c}{GA_{c_{(i-1)}}} + \frac{h_{(i-1)}c^3}{12EI_{c_{(i-1)}}}\right) = T'_i\big|_{z=z_i}\left(\frac{1.2h_i c}{GA_{c_i}} + \frac{h_i c^3}{12EI_{c_i}}\right)$$

$$(i = 2,3,...,n) \tag{57}$$

7- Since the total twisting moments of the two neighbouring regions (i) and (i–1), at height $z = z_i$ balance each other

$$\left[M_{Et_{(i-1)}} - M_{Et_i}\right] + \left[-EI_{\theta Y}u'''_{(i-1)} + EI_{\theta Y}u'''_i\right]$$

$$+ \left[EI_{\theta X}v'''_{(i-1)} - EI_{\theta X}v'''_i\right] + \left[-GJ\theta'_{(i-1)} + GJ\theta'_i\right]$$

$$+ \left[EI_\omega\theta'''_{(i-1)} - EI_\omega\theta'''_i\right] + \left[(\omega + d)T'_{(i-1)} - (\omega + d)T'_i\right] = 0 \tag{58}$$

Expressing all unknown functions in terms of T_i and its derivatives, after some rearrangements, the seventh type boundary condition is found as:

$$C_{1(i-1)}T'''_{(i-1)} - C_{1i}T'''_i + C_{2(i-1)}T'_{(i-1)} - C_{2i}T'_i + C_{3(i-1)} - C_{3i} = 0$$

$$(i = 2,3,...,n) \tag{59}$$

where

$$C_{1i} = \frac{\gamma_i K_1 I_{\theta Y}}{r} + \frac{\gamma_i K_2 I_{\theta X}}{r} - \frac{I_\omega \gamma_i}{r}$$

$$C_{2i} = I_{\theta Y}K_3 - I_{\theta X}K_4 - \frac{I_{\theta Y}K_1}{Ar} - \frac{I_{\theta X}K_2}{Ar} + \frac{I_\omega}{Ar} + \omega + d$$

$$C_{3i} = \left(\frac{I_{XY}I_{\theta Y}M'_{EX_i} + I_Y I_{\theta X}M'_{EX_i}}{\Delta}\right) - \left(\frac{I_{XY}I_{\theta X}M'_{EY_i} + I_X I_{\theta Y}M'_{EY_i}}{\Delta}\right)$$

$$- \left(\frac{I_\omega - I_{\theta Y}K_1 - I_{\theta X}K_2}{r}\right)\left(\frac{K_4 M'_{EX_i} + K_3 M'_{EY_i}}{r}\right) + M_{Et_i} \tag{60}$$

8-Since the total bimoments of the two neighbouring regions (i) and (i–1), at height $z = z_i$ balance each other

$$\left[B_{E_{(i-1)}} - B_{E_i}\right] + \left[-EI_{\theta Y}u''_{(i-1)} + EI_{\theta Y}u''_i\right] + \left[EI_{\theta X}v''_{(i-1)} - EI_{\theta X}v''_i\right]$$
$$+ \left[EI_{\omega}\theta''_{(i-1)} - EI_{\omega}\theta''_i\right] + \left[(\omega + d)T_{(i-1)} - (\omega + d)T_i\right] = 0 \qquad (61)$$

Expressing the other unknown functions in terms of T_i and its derivatives, after some necessary rearrangements, the eighth type boundary condition is obtained as:

$$C_{1(i-1)}T''_{(i-1)} - C_{1i}T''_i + C_{2(i-1)}T_{(i-1)} - C_{2i}T_i + C_{4(i-1)} - C_{4i} = 0 \qquad (62)$$

Where

$$C_{4i} = \left(\frac{I_{XY}I_{\theta Y}M_{EX_i} + I_Y I_{\theta X}M_{EX_i}}{\Delta}\right) - \left(\frac{I_{XY}I_{\theta X}M_{EY_i} + I_X I_{\theta Y}M_{EY_i}}{\Delta}\right)$$
$$- \left(\frac{I_{\omega} - I_{\theta Y}K_1 - I_{\theta X}K_2}{r}\right)\left(\frac{K_4 M_{EX_i} + K_3 M_{EY_i}}{r}\right) + B_{E_i} \qquad (63)$$

To determine the integration constants D_{1i} to D_{4i}, the boundary conditions at the top, bottom and between each pair of consecutive regions are used. Substituting them in expression (45), the general solution for T_i $(i = 1,2,\ldots,n)$ can be found.

Determination of lateral displacements and rotation functions

The lateral displacement and rotation functions (u_i, v_i, and θ_i) can be found using (13-14,40) as follows:

$$\theta_i = \frac{1}{Er}\int\left(\int\left[-M_{EX_i}K_3 - M_{EX_i}K_4 + \frac{T_i}{A} - T''_i\gamma_i\right]dz\right)dz + G_{1i}z_i + G_{2i} \qquad (64)$$

$$u_i = \frac{1}{E}\int\left(\int\left[E\theta''_i K_1 - T_i K_3 - \frac{M_{EX_i}I_{XY}}{\Delta} + \frac{M_{EY_i}I_X}{\Delta}\right]dz\right)dz + R_{1i}z_i + R_{2i} \qquad (65)$$

$$v_i = \frac{1}{E}\int\left(\int\left[-E\theta''_i K_2 - T_i K_4 - \frac{M_{EY_i}I_{XY}}{\Delta} + \frac{M_{EX_i}I_Y}{\Delta}\right]dz\right)dz + N_{1i}z_i + N_{2i} \qquad (66)$$

where boundary conditions (49) and the equivalence of the horizontal displacements and the respective slopes for every pair of neighbouring regions at their common boundary ($z = z_i$) are used to determine the integration constants.

Numerical results

In the example, the behaviour of the coupled shear wall with four stiffening beams in Figures 12-13 is examined. Stiffening beams of 3.0 m height are placed at the levels of ninth, thirteenth and seventeenth stories and a last one with 2.0 m height at the top, as seen in Figure 12.

The sectorial area diagram of the cross-section of the structure is given in Figure 14. The structure is solved both by the present method using the CCM and by the SAP2000 structural analysis program (Wilson, 1997) using the frame method (MacLeod, 1977), for which the model and its 3-D view are given in Figure 15.

The geometrical properties and the cross-sectional view of the structure are given in Figures 12-13. The total height of the shear wall is 72 m, the storey height is 3 m and the thicknesses of the piers and the connecting beams are shown in Figure 13. The height of the connecting beams is 0.4m and the elasticity and shear-moduli are $E=2.85\times10^6$ kN/m^2 and G=1055556 kN/m^2, respectively. The external loads act at the top of the structure as shown in Figures 12-13. The lateral displacements at points on Z axis and the rotations, found by the present program and the SAP2000 structural analysis program, are compared, for the unstiffened and stiffened cases, in Figures 16-17.

Conclusions

In this study, non-planar shear walls coupled with connecting and stiffening beams are analyzed under lateral loading. The analysis is performed using Vlasov's thin-walled beam theory in conjunction with the CCM.

In the example, the behaviour of a coupled shear wall with four stiffening beams is examined. The results obtained have been compared with those of SAP2000 and a good agreement has been observed.

As seen in Figures 16-17, the stiffening of coupled shear walls cause a decrease in the maximum displacement at the top and the maximum bending moment at the bottom of a building. Thus, by using such stiffening beams the heights of buildings can be increased more. The stiffening of coupled shear walls is realized by placing high connecting beams at the levels of whole or partial stories used as storage or service areas. The number and levels of these high beams, to improve the structural behaviour of the buildings, is up to the design engineer.

The method proposed in this study, has two main advantages, which are that the data preparation is much easier compared to the equivalent frame method for non-planar coupled shear walls and the computation time needed is much shorter compared to other methods. Hence, the method presented in this study is very useful for predesign purposes while determining the dimensions of non-planar coupled shear wall structures.

ACKNOWLEDGEMENTS

The financial support of the Scientific Research Projects Unit of Akdeniz University is gratefully acknowledged.

Nomenclature: a, distance between the centroids of the piers in X direction; A_j cross sectional area of the j^{th} pier; A_{c_i}, cross sectional area of connecting beams in region i; b, distance between the centroids of the piers in Y direction; B, Bimoment;

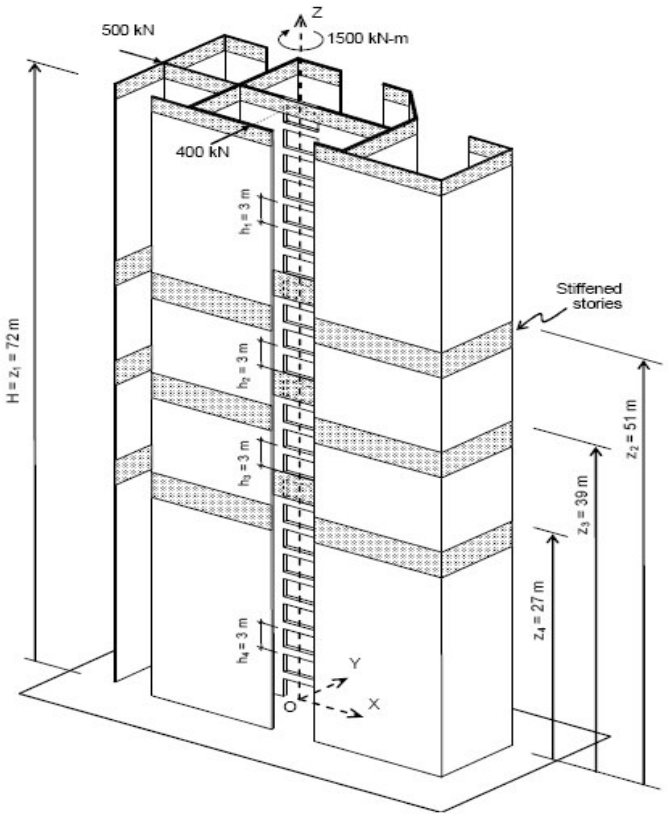

Figure 12. Non-planar asymmetrical example structure.

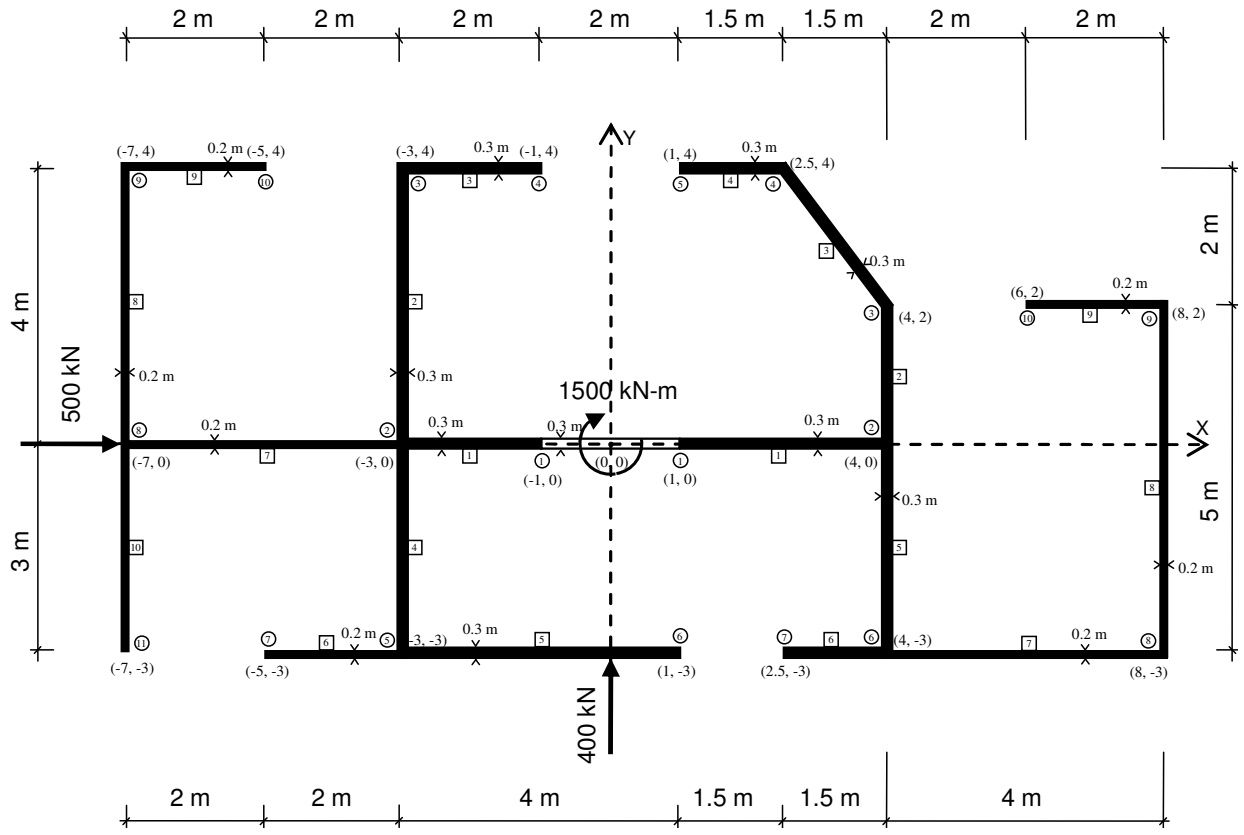

Figure 13. Cross-sectional view of the example structure.

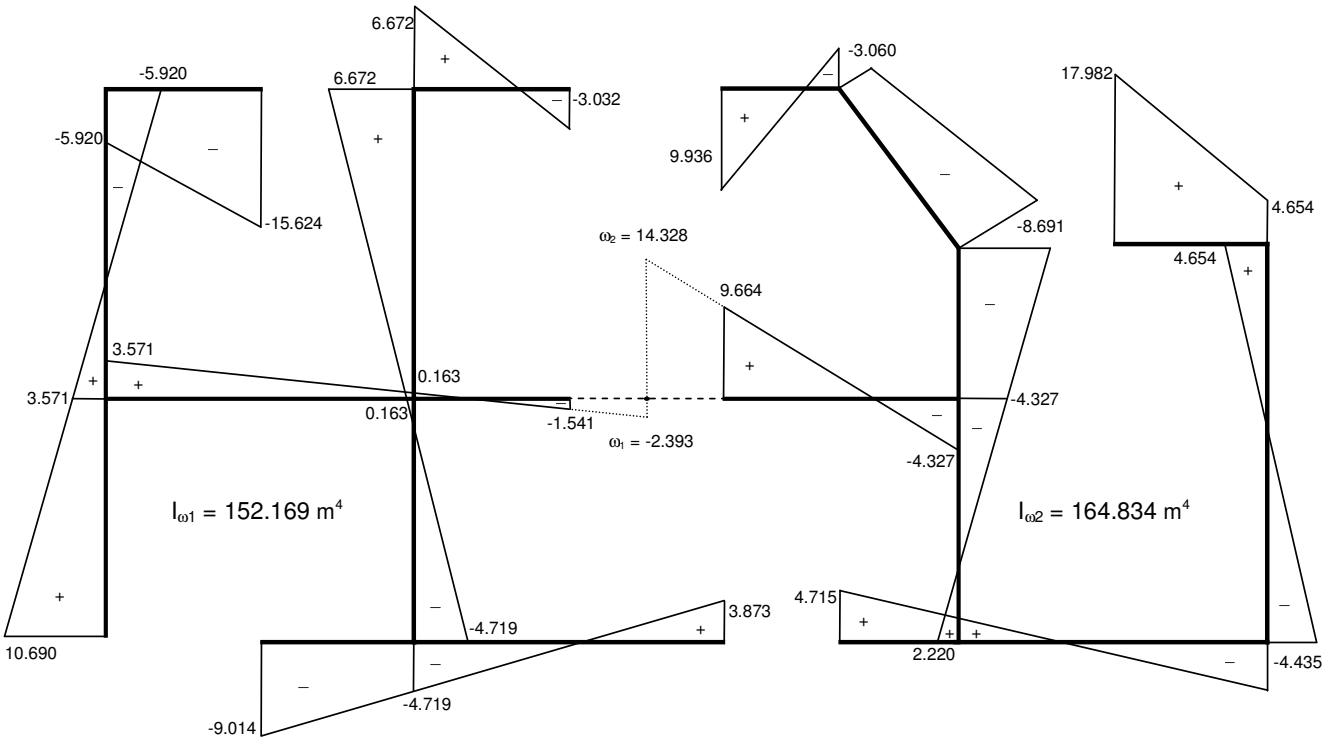

Figure 14. The principal sectorial area diagram of the cross-section.

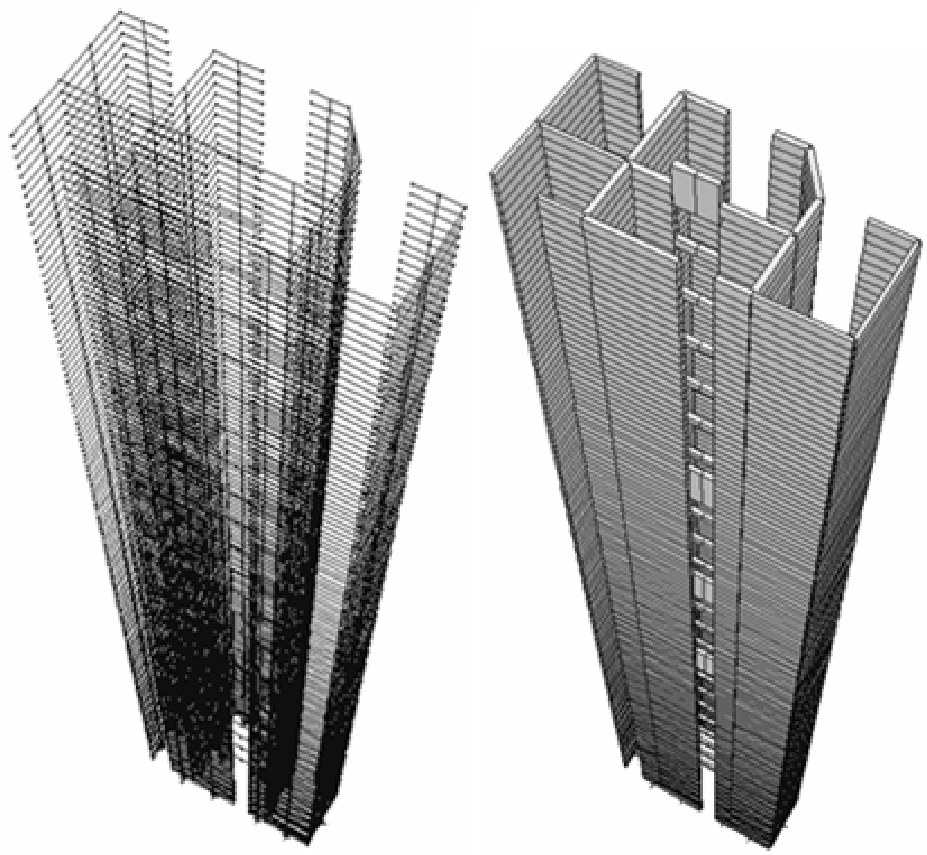

Figure 15. Frame model of the example structure and its 3-D view.

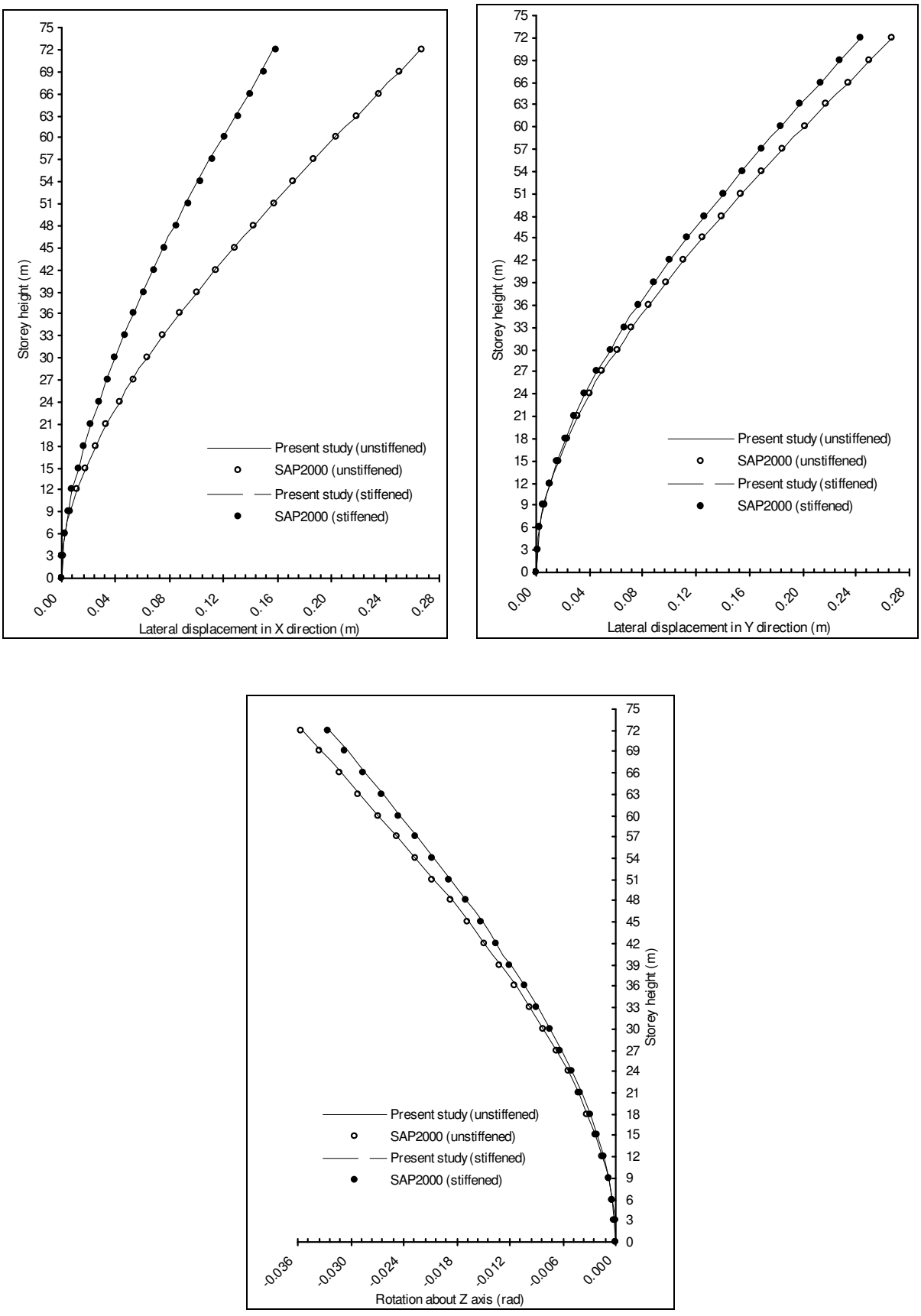

Figure 16. Comparison of the lateral displacements and rotations.

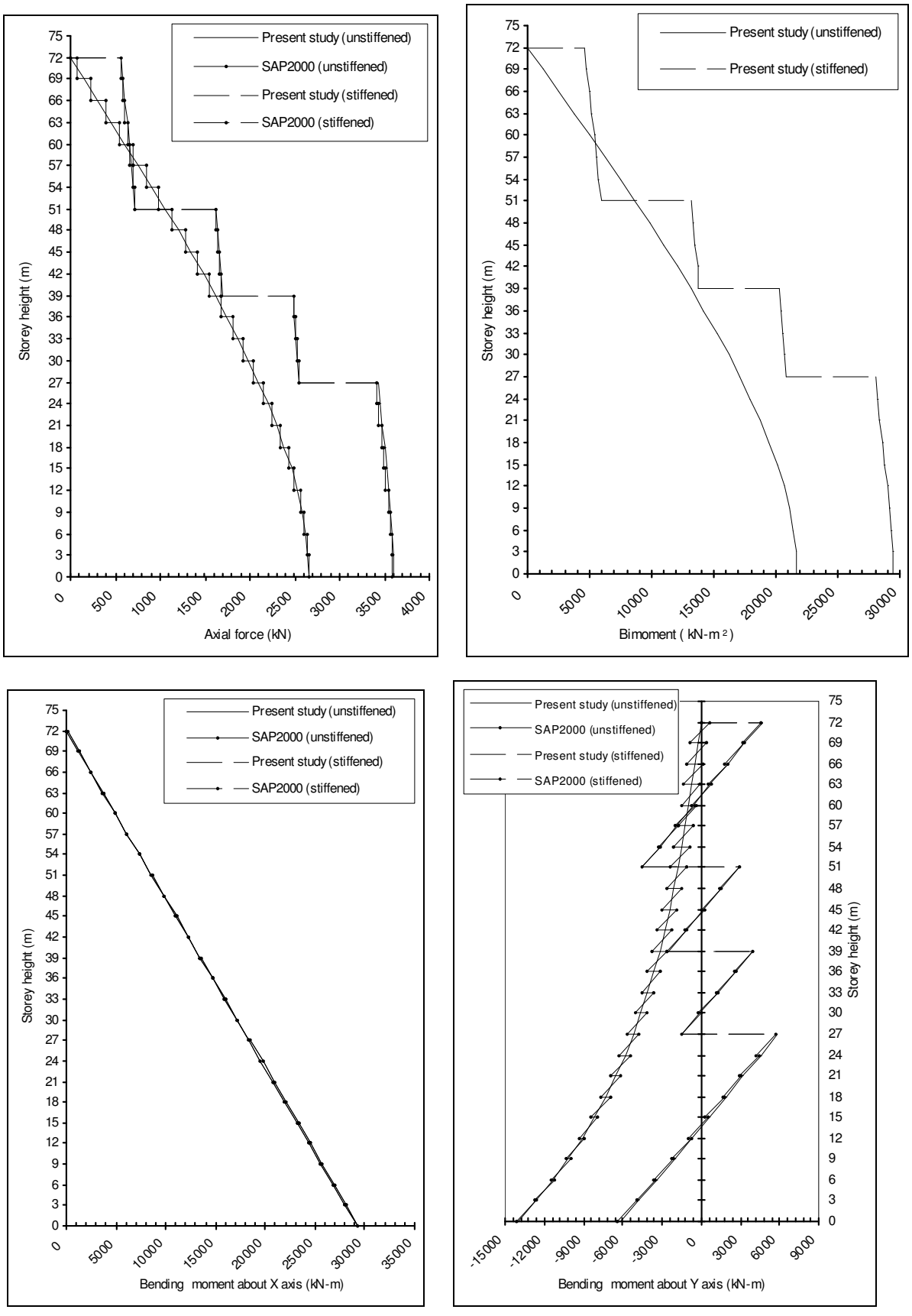

Figure 17. The axial forces, the total bimoments and the total shear wall bending moments along the height.

B_{E_i}, external bimoment value; $\overline{B_i}$, resultant bimoment, about Z axis, due to the resistance offered by the piers in region i; $\overline{\overline{B_i}}$ resultant bimoment, about Z axis, due to the component bending moments and bimoments in region i; d, a geometric property; d_{PX}, d_{PY}, moment arms of the components of the concentrated force; d_{WX}, d_{WY}, moment arms of the distributed force components; **E,** elasticity modulus; **G,** shear modulus; x_{g_j}, y_{g_j}, coordinates of the centroid of j^{th} pier, referring to global axes, X and Y, respectively; $\overline{x_{g_j}}, \overline{y_{g_j}}$, coordinates of centroid of the j^{th} pier, referring to principal axes, $\overline{X}$ **and** $\overline{Y}$, respectively; H, total height of shear wall; h_i, storey height in region i; i, region number; I_{c_i}, moment of inertia of connecting beams in region i; I_{x_j}, I_{y_j}, moments of inertia of pier j w.r.t. global X and Y axes, respectively; I_{xy_j}, product of inertia of pier j w.r.t. global X and Y axes in region i; $\overline{I_{x_j}}, \overline{I_{y_j}}$, moments of inertia of pier j w.r.t. principal $\overline{X}$ and $\overline{Y}$ axes, respectively; $\overline{I_{xy_j}}$, product of inertia of pier j w.r.t. principal $\overline{X}$ and $\overline{Y}$ axes; I_{ω_j}, sectorial moment of inertia of pier j; I_ω, sum of the sectorial moments of inertia of the two piers at the point on Z axis; $\overline{I_\omega}$, a geometrical constant; $I_{\theta X}, I_{\theta Y}$, sectional properties; j, pier number; J_j, St. Venant torsional constant (moment of inertia) of pier j; j, sum of the St. Venant torsional constants of the two piers; K_1, K_2, K_3, K_4, geometrical quantities related to moments of inertia; M_{EX_i}, M_{EY_i}, external bending moments in region i about the respective axes due to the loading above the cross-section considered; M_{Et_i}, external twisting moment in region i due to the loading above the cross-section considered; $\overline{M_{t_i}}$, resultant torque, about Z axis, due to resistance offered by piersin region i; $\overline{\overline{M_{t_i}}}$, resultant torque, about Z axis, due to component shears and torques in region i; N, number of regions in vertical direction; O(X,Y,Z), orthogonal system of global axes; P_X, P_Y, concentrated forces in X and Y directions, respectively; $Q_{x_{ji}}, Q_{y_{ji}}$, shear forces developed in a region due to shear flow, q_i, in the laminae; q_i, shear flow in laminae per unit length in region i; R, a geometrical constant; S_j, shear center of j^{th} pier; x_{s_j}, y_{s_j}, coordinates of the shear center of the j^{th} pier, referring to global axes, X and Y, respectively; T_i, axial force in region i; T, thickness of a thin-walled beam; u_x, u_y, u_z, displacement components in the directions of orthogonal global system of axes O(X,Y,Z); u_i, horizontal global displacement of the point on Z axis in X direction in region i; u_{ji}, horizontal principal displacement of the center of j^{th} pier in $\overline{X_{ji}}$ direction in region i; v_i, horizontal global displacement of the point on Z axis global X and Y axes, respectively; I_{xy_j}, product of inertia of pier j w.r.t. global X and Y axes in region i; $\overline{I_{x_j}}, \overline{I_{y_j}}$, moments of inertia of pier j w.r.t. principal $\overline{X}$ and $\overline{Y}$ axes, respectively; $\overline{I_{xy_j}}$, product of inertia of pier j w.r.t. principal $\overline{X}$ and $\overline{Y}$ axes; I_{ω_j}, sectorial moment of inertia of pier j; I_ω, sum of the sectorial moments of inertia of the two piers at the point on Z axis; $\overline{I_\omega}$, a geometrical constant; $I_{\theta X}, I_{\theta Y}$, sectional properties; j, pier number; J_j, St. Venant torsional constant (moment of inertia) of pier j; j, sum of the St. Venant torsional constants of the two piers; K_1, K_2, K_3, K_4, geometrical quantities related to moments of inertia; M_{EX_i}, M_{EY_i}, external bending moments in region i about the respective axes due to the loading above the cross-section considered; M_{Et_i}, external twisting moment in region i due to the loading above the cross-section considered; $\overline{M_{t_i}}$, resultant torque, about Z axis, due to resistance offered by piersin region i; $\overline{\overline{M_{t_i}}}$, resultant torque, about Z axis, due to component shears and torques in region i; N, number of regions in vertical direction; O(X,Y,Z), orthogonal system of global axes; P_X, P_Y, concentrated forces in X and Y directions, respectively; $Q_{x_{ji}}, Q_{y_{ji}}$, shear forces developed in a region due to shear flow, q_i, in the laminae; q_i, shear flow in laminae per unit length in region i; R, a geometrical constant; S_j, shear center of j^{th} pier; x_{s_j}, y_{s_j}, coordinates of the shear center of the j^{th} pier, refering to global axes, X and Y, respectively; T_i, axial force in region i; T, thickness of a thin-walled beam; u_x, u_y, u_z, displacement components in the directions of orthogonal global system of axes O(X,Y,Z); u_i, horizontal global displacement of the point on Z axis in X direction in region i; u_{ji}, horizontal principal displacement of the center of j^{th} pier in $\overline{X_{ji}}$ direction in region i; v_i, horizontal global displacement of the point on Z axisin Y direction in region i; v_{ji}, horizontal principal displacement of the center of j^{th} pier in $\overline{Y_{ji}}$ direction in region i; V_i, shear force in i^{th} stiffening beam; Z, spatial coordinate measured along the height of the structure; W_X, uniform load in X direction; W_Y, uniform load in Y direction; β_{1i}, β_{2i}, β_{3i}, geometrical constants; δ_{1i}, the relative vertical displacement due to the bending of the piers in $\overline{X}$ and $\overline{Y}$ directions and due to the warping of the piers; δ_{2i}, the relative vertical displacement due to the axial deformation of the piers caused by the induced axial forces arising from the shear flow q_i in the connecting medium; δ_{3i}, the relative vertical displacement due to the bending of the connecting beams; δ_{4i}, the relative vertical displacement due to the shear deformations in the laminae; θ_I, rotational global displacement of the rigid diaphragm in region i; θ_{ji}, rotational principal displacement of j^{th} pier about $\overline{Z_{ji}}$ direction in region i; θ'_z, angle of twist per unit length; ω_j, sectorial area of pier j at the point on Z axis; ϕ_j, angle between the global axes and the principal axes of j^{th} pier; γ_i, a constant property of connecting beams; Δ, a geometrical constant.

REFERENCES

Aksogan O, Bikce M, Emsen E, Arslan HM (2007). A simplified dynamic analysis of multi-bay stiffened coupled shear walls. Adv. Eng. Software. 38: 552-560.

Aksogan O, Turker HT, Oskouei AV (1993). Stiffening of coupled shear walls at arbitrary number of heights. First Technical Congress on Advances in Civil Engineering. North Cyprus: 2: 780-787.

Arslan HM, Aksogan O, Choo BS (2004). Free vibrations of flexibly connected elastically supported stiffened coupled shear walls with stepwise changes in width. Iranian J. Sci. Technol. 28(B5): 605-614.

MacLeod IA, Hosny HM (1977). Frame analysis of shear wall cores. J. Structl Div. ASCE. 103(10): 2037-2045.

Rosman R (1964). Approximate analysis of shear walls subject to lateral loads. J. Am. Concrete Inst. 61(6): 717-732.

Tso WK, Biswas JK (1973). General analysis of non-planar coupled shear walls. J. Struct. Div. ASCE. 100(ST5): 365-380.

Vlasov VZ (1961). Thin-walled elastic beam. Washington DC: US Department of Commerce, pp. 1-2.

Wilson EL (1997). SAP2000 Integrated finite element analysis and design of structures. USA: Computers and Structures, Inc.

Zbirohowski-Koscia K (1967). Thin-walled beams from theory to practice. London: Crosby Lockwood Staples.